Localization of Near-Field Signals Based on Linear Prediction and Oblique Projection Operator

Wenyi Liu[†‡], Weiliang Zuo[†‡], Jingmin Xin[†‡], Nanning Zheng[†‡], Akira Sano[§]
[†] Institute of Artificial Intelligence and Robotics, Xi'an Jiaotong University, Xi'an 710049, China
[‡] National Engineering Laboratory for Visual Information Processing and Applications,
Xi'an Jiaotong University, Xi'an 710049, China
[§] Department of System Design Engineering, Keio University, Yokohama 223-8522, Japan

***Abstract*—Recently many subspace-based localization methods were developed for estimating the directions of arrivals (DOAs) and ranges of multiple narrowband signals in near-field. However, most of them usually encounter "saturation behavior" in estimation performance regardless of the signal-to-noise ratio (SNR) when the number of array snapshots is not sufficiently large enough. In this paper, we investigate the problem of localizing multiple narrowband near-field signals impinging on a symmetrical uniform linear array (ULA). Firstly, by exploiting the anti-diagonal elements of the array covariance matrix, a new linear prediction approach with truncated singular value decomposition (SVD) is proposed to estimate the location parameters (i.e., DOA and range) of the incident signals. Secondly, as a measure against the impact of finite array data, an alternating iterative scheme is presented to improve the estimation accuracy of the location parameters, where the "saturation behavior" encountered in most of localization methods is solved effectively. Furthermore, the statistical analysis of the proposed method is studied, and the asymptotic mean-squared-error (MSE) expressions of the estimation errors are derived for two location parameters. Finally, the effectiveness and the theoretical analysis are substantiated through numerical examples.**

I. Introduction

Localization of multiple narrowband near-field signals impinging on an array of sensors has various important applications in sonar, radar, seismology, speech enhancement, and biomedical imaging (e.g., [1]– [6]), where the signal source is close to the array and lies in the near-field (i.e., the Fresnel region), and hence the wave impinging on the array has spherical wavefront, which is characterized by two independent location parameters (i.e., direction of arrival (DOA) and range). As a result, numerous conventional estimation methods with the far-field assumption parameterized only by the DOA (e.g., [7], [8]) generally are no longer applicable in the near-field situation, and the pair-matching of the estimated DOAs and ranges is usually required.

In fact, by considering its second-order Taylor expansion to approximate the spherical wavefront (i.e., Fresnel approximation), many localization methods were proposed for the near-field narrowband signals. Some high-order statistics (HOS) or cyclostationarity based localization methods have been presented for near-field signal with specifically temporal properties [6], [9]–[11], while maximum likelihood estimation (MLE) methods were studied in [12], [13]. But they often require many array snapshots and have high computational load. Additionally, the path-following method [14], the tensor-based method [15], and the generalized ESPRIT based method [16] were suggested. Especially, by taking advantages of some designated characteristics of the second-order statistics (SOS) of the observed array data, a weighted linear prediction method (WLPM) was proposed for the near-field signals impinging on a symmetrical uniform linear array (ULA) [17]. Unfortunately, when the number of array snapshots is not sufficiently large enough, most of the existing localization methods usually encounter "saturation behavior" in estimation performance regardless of the signal-to-noise ratio (SNR), where the estimated DOAs and ranges have high level of errors, which do not decrease monotonically with the increasing SNR.

Therefore, the purpose of this paper is to investigate the problem of localizing multiple narrowband near-field signals impinging on a symmetrical ULA. Firstly, by exploiting the anti-diagonal elements of the array covariance matrix, a new linear prediction (LP) approach with truncated singular value decomposition (SVD) is proposed to estimate the location parameters (i.e., DOA and range) of the incident signals. Then by introducing the oblique projection operator [19], an alternating iterative scheme is presented as a measure against the impact of finite array data, where the estimation accuracy of the location parameters (i.e., DOAs and ranges) is improved, and consequently the aforementioned "saturation behavior" is overcome. Furthermore, the statistical analysis of the proposed method is studied, and the asymptotic mean-squared-error (MSE) expressions of the estimation errors are derived for two location parameters. Finally, the effectiveness and the theoretical analysis are verified through numerical examples.

II. Data Model

We consider K narrowband noncoherent signals $\{s_k(n)\}$ in near-field and imping on a ULA consisting of $2M+1$ sensors with spacing d. By letting the center of the array be the phase reference point, the received noisy signal $x_m(n)$ at the m-th

This work was supported in part by the National Natural Science Foundation of China under Grants 61671373 and 61790563, and the Programme of Introducing Talents of Discipline to Universities under Grant B13043.

sensor can be expressed as

$$x_m(n) = \sum_{k=1}^{K} s_k(n) e^{j\tau_{mk}} + w_m(n) \tag{1}$$

where $m = -M, \cdots, M$, $w_m(n)$ is the additive noise, and τ_{mk} is the phase delay due to the time delay between the reference sensor and the m-th sensor for the k-th signal, which is given by [5]

$$\tau_{mk} = \frac{2\pi}{\lambda}\left(\sqrt{r_k^2 + (md)^2 - 2r_k md \sin\theta_k} - r_k\right) \tag{2}$$

where θ_k and r_k are the DOA and range of the kth signal, and λ is the wavelength. When the k-th signal is in the Fresnel region (i.e., $r_k \in (0.62(D^3/\lambda)^{1/2}, 2D^2/\lambda)$, where D is the aperture of the array [2], τ_{mk} can be approximated by using the second-order Taylor expansion as [17], [18]

$$\tau_{mk} \approx \psi_k m + \phi_k m^2 \tag{3}$$

where $\psi_k \triangleq -2\pi d \sin\theta_k/\lambda$, $\phi_k \triangleq \pi d^2 \cos^2\theta_k/(\lambda r_k)$, and they are called electric angles since they map the real parameters to a simpler form. Thus, the received signals vector $\boldsymbol{x}(n) \triangleq [x_{-M}(n), x_{-M+1}(n), \cdots, x_{M-1}(n), x_M(n)]^T$ can be rewritten in a vector-matrix form as

$$\begin{aligned}\boldsymbol{x}(n) &= \sum_{k=1}^{K} \boldsymbol{a}(\theta_k, r_k) s_k(n) + \boldsymbol{w}(n) \\ &= \boldsymbol{A}\boldsymbol{s}(n) + \boldsymbol{w}(n)\end{aligned} \tag{4}$$

where $(\cdot)^T$ denotes transpose, $\boldsymbol{s}(n)$ and $\boldsymbol{w}(n)$ are the vectors of incident signals and additive noises given by $\boldsymbol{s}(n) \triangleq [s_1(n), s_2(n), \cdots, s_K(n)]^T$ and $\boldsymbol{w}(n) \triangleq [w_{-M}(n), w_{-M+1}(n), \cdots, w_{M-1}(n), w_M(n)]^T$, while $\boldsymbol{A}$ is the steering matrix of the calibrated ULA defined by $\boldsymbol{A} \triangleq [\boldsymbol{a}(\theta_1, r_1), \boldsymbol{a}(\theta_2, r_2), \cdots, \boldsymbol{a}(\theta_K, r_K)]$, and $\boldsymbol{a}(\theta_k, r_k)$ is the array steering vectors which can be expressed as

$$\begin{aligned}\boldsymbol{a}(\theta_k, r_k) \triangleq [&e^{-jM\psi_k + jM^2\phi_k}, \cdots, e^{-j\psi_k + j\phi_k}, 1, \\ &e^{j\psi_k + j\phi_k}, \cdots, e^{jM\psi_k + jM^2\phi_k}]^T.\end{aligned} \tag{5}$$

In this paper, we assume that the array response matrix $\boldsymbol{A}$ is full rank (i.e., rank$\{\boldsymbol{A}\} = K$). The incident signals $\{s_k(n)\}$ are zero-mean wide-sense stationary random processes, while the additive noises $\{w_m(n)\}$ are uncorrelated with the incident signals and are temporally and spatially complex white Gaussian random process with zero-mean and variance σ^2. Additionally the numbers of the incident signals K is known and $K \leq M$.

III. Localization Based Linear Prediction Approach with Truncated SVD

Under the basic assumption and data model, the covariance matrix $\boldsymbol{R}$ of the array output is given by

$$\boldsymbol{R} = E\{\boldsymbol{x}(n)\boldsymbol{x}(n)^H\} = \boldsymbol{A}\boldsymbol{R}_s\boldsymbol{A}^H + \sigma^2 \boldsymbol{I}_{2M+1} \tag{6}$$

By letting $\bar{\boldsymbol{r}}_i$ denote the vector that consists of the ith anti-diagonal elements of covariance matrix $\boldsymbol{R}$ and $i = 0, \pm1, \cdots, \pm 2M$, the pth element of $\bar{\boldsymbol{r}}_i$ is defined by

$$\begin{aligned}\bar{r}_i(p) &\triangleq E\{x_{p-i}(n) x^*_{-p}(n)\} \\ &= \sum_{k=1}^{K} r_{s_k} e^{j(2p-i)(\psi_k - i\phi_k)} + \sigma^2 \delta(2p - i)\end{aligned} \tag{7}$$

for $p = -M + i_-, \cdots, M - i_+$, where $i_- \triangleq \frac{1}{2}(|i| + i)$, $i_+ \triangleq \frac{1}{2}(|i| - i)$, r_{s_k} is the power of the kth signal $s_k(n)$, $\delta(\cdot)$ is the Kronecker delta, and $(\cdot)^*$ denotes the complex conjugate. Obviously

$$\bar{r}_i^*(p) = \bar{r}_i(-p + i) \tag{8}$$

By partitioning the matrix $\boldsymbol{R}$ in (6) as

$$\boldsymbol{R} = \begin{array}{c} \quad K \qquad 2M+1-K \\ \left[\begin{array}{cc} \boldsymbol{R}_{11}, & \boldsymbol{R}_{12} \\ \boldsymbol{R}_{21}, & \boldsymbol{R}_{22} \end{array}\right] \begin{array}{l} K \\ 2M+1-K \end{array}\end{array} \tag{9}$$

we have the noise variance σ^2 from $\boldsymbol{R}_{21}$ and $\boldsymbol{R}_{22}$ as [22]

$$\sigma^2 = \frac{\mathrm{tr}\{\boldsymbol{R}_{22}\boldsymbol{\Pi}\}}{\mathrm{tr}\{\boldsymbol{\Pi}\}} \tag{10}$$

where $\boldsymbol{\Pi} = \boldsymbol{I}_{2M+1-K} - \boldsymbol{R}_{21}\boldsymbol{R}_{21}^\dagger$, and $\boldsymbol{R}_{21}^\dagger = (\boldsymbol{R}_{21}^H \boldsymbol{R}_{21})^{-1} \cdot \boldsymbol{R}_{21}^H$. In the following, we will use $r_i(p)$ to stand for its corresponding noise-free correlation, i.e., $r_i(p) = \bar{r}_i(p) - \sigma^2\delta(2p - i)$.

A. Truncated SVD-based Linear Prediction Estimation

By dividing the vector $\boldsymbol{r}_i$ into L overlapping forward vectors with q elements, where $q > K + 1$ and $L = 2M + 2 - q - |i|$, the entry $r_i(M - b_+ - l - 1)$ can be predicted from a linear combination of the other entries as [23]

$$r_i(M - i_+ - l + 1) = \boldsymbol{a}_i^T \boldsymbol{r}_{i, M-i_+-l-q+2} \tag{11}$$

where $\boldsymbol{r}_{i,M-i_+-l-q+2} = [r_i(M-i_+-l-q+2), r_i(M-i_+-l-q+3), \cdots, r_i(M-i_+-l)]^T$, $\boldsymbol{a}_i = [a_{i,q-1}, a_{i,q-2}, \cdots, a_{i,1}]^T$, in which $\{a_{i,i}\}$ and q are the coefficients and the order of the LP model. Specifically, from (11), we have a matrix-vector form as

$$\boldsymbol{R}_i \boldsymbol{a}_i = \boldsymbol{g}_i \tag{12}$$

where the $L \times (q - 1)$ matrix $\boldsymbol{R}_i$ are given by

$$\boldsymbol{R}_i = \left[\boldsymbol{r}_{i,M-i_+-q+1}, \boldsymbol{r}_{i,M-i_+-q}, \cdots, \boldsymbol{r}_{i,-M+i_-}\right]^T \tag{13}$$

and $\boldsymbol{g}_i = [r_i(M - i_+), r_i(M - i_+ - 1), \cdots, r_i(-M + i_- + q - 1)]^T$. Clearly, $\boldsymbol{a}_i = \boldsymbol{R}_i{}^\dagger \boldsymbol{g}_i$, where $(\cdot)^\dagger$ stands for pseudoinverse. However, as it was pointed out in [20] that $\boldsymbol{R}_i$ can be replaced by a low rank approximate before performing the pseudoinverse. For this purpose, by taking the singular value decomposition (SVD) of matrix $\boldsymbol{R}_i$ as

$$\boldsymbol{R}_i = \boldsymbol{U}_i \boldsymbol{\Lambda}_i \boldsymbol{V}_i{}^H \tag{14}$$

where $(\cdot)^H$ represents Hermitian transposition, $\boldsymbol{U}_i = [\boldsymbol{u}_{i,1}, \boldsymbol{u}_{i,2}, \cdots, \boldsymbol{u}_{i,q-1}]$, $\boldsymbol{V}_i = [\boldsymbol{v}_{i,1}, \boldsymbol{v}_{i,2}, \cdots, \boldsymbol{v}_{i,q-1}]$, and $\boldsymbol{\Lambda}_i =$

ISBN 978-90-827970-1-5 © EURASIP 2018

$\mathrm{diag}(\lambda_{i,1}, \lambda_{i,2}, \cdots, \lambda_{i,q-1})$, then we have the minimum-norm estimation of the LP parameter with the truncated SVD as [20], [21], [23], [24]

$$\boldsymbol{a}_i = \sum_{k=1}^{K} \frac{\boldsymbol{u}_{i,k}\boldsymbol{v}_{i,k}^H}{\lambda_{i,k}} \boldsymbol{g}_i \tag{15}$$

where the principal eigenvalues $\lambda_{i,1} \geq \lambda_{i,2} \geq \cdots \geq \lambda_{i,K} \geq \lambda_{i,K+1} = \cdots = \lambda_{i,q-1} = 0$. Hence, a prediction polynomial $D_i(z)$ can be formed as [20], [21], [23], [24],

$$D_i(z) = 1 - a_{i,1}z^{-1} - \cdots - a_{i,q-1}z^{-(q-1)} \tag{16}$$

where $z = e^{2j(\psi_k - b\phi_k)}$, and the electric angles ψ_k and ϕ_k of the near-field signals can be estimated from the K signal zeros of $D(z)$ closest to the unit circle in the z-plane.

Apparently, under the assumption that $K \leq M$, we can form at least three groups of LP equations corresponding to $i = 0, 1$ and -1 providing estimates of $\{\psi_k\}$, $\{\psi_k - \phi_k\}$, and $\{\psi_k + \phi_k\}$. Finally by using the parameter pairing procedure [17], we have

$$\psi_k = \frac{1}{2}\{(\phi_k + \psi_k) - (\phi_k - \psi_k)\} \tag{17}$$

$$\phi_k = \frac{1}{2}\{(\phi_k + \psi_k) + (\phi_k - \psi_k)\} \tag{18}$$

Then, the estimated location parameters $\hat{\theta}_k$ and $\hat{r}_k$ of each near-field signal can be obtained.

IV. Oblique Projection Based Alternating Iteration for Performance Improvement

A. Saturation in Near-Field Localization

In practice, the matrix $\boldsymbol{R}$ should be estimated from finite received array data and can be expressed as

$$\begin{aligned}\hat{\boldsymbol{R}} &= \frac{1}{N}\sum_{n=1}^{N} \boldsymbol{x}(n)\boldsymbol{x}^H(n) \\ &= \boldsymbol{A}\hat{\boldsymbol{R}}_s\boldsymbol{A}^H + \boldsymbol{A}\hat{\boldsymbol{R}}_{sw} + \hat{\boldsymbol{R}}_{sw}^H\boldsymbol{A}^H + \hat{\boldsymbol{R}}_w \end{aligned}\tag{19}$$

where $\hat{\boldsymbol{R}}_s = (1/N)\sum_{n=1}^N \boldsymbol{s}(n)\boldsymbol{s}^H(n)$, $\hat{\boldsymbol{R}}_{sw} = (1/N) \sum_{n=1}^N \boldsymbol{s}(n)\boldsymbol{w}^H(n)$, and $\hat{\boldsymbol{R}}_w = (1/N)\sum_{n=1}^N \boldsymbol{w}(n)\boldsymbol{w}^H(n)$. Obviously when the number of snapshots N is not sufficiently large enough, the second and third terms in above will not decrease monotonically with the increasing SNR. Furthermore, $\hat{\boldsymbol{R}}_s$ and $\hat{\boldsymbol{R}}_w$ will not be strictly diagonal. Consequently, the estimated elements $\{\hat{\bar{r}}_i(p)\}$ in the ith cross-diagonal of $\hat{\bar{\boldsymbol{R}}}$ will not just contain information of $\psi_k - i\phi_k$. Hence the "saturation behavior" will be encountered in the localization of near-field signals regardless of the SNR, where the estimated DOA and range (i.e, $\hat{\theta}_k$ and $\hat{r}_k$) may have high elevated error floors, which do not decrease monotonically with the increasing SNR.

B. Alternating Iteration with Oblique Projection Operator

The range space of each incident signal is nonoverlapping and not orthogonal to that of another signal, here we consider the utilization of oblique projection operator [19] to isolate one incident signal from the others and to eliminate their mutual interference between the signals. Firstly, estimate the electric angles of the near-field signals with (16) and denote them as $\{\hat{\psi}_k^{(i)}\}_{k=1}^K$ and $\{\hat{\phi}_k^{(i)}\}_{k=1}^K$. Secondly, divide the range space of the estimated steering matrix $\hat{\boldsymbol{A}}$ as follows

$$\mathcal{R}(\hat{\boldsymbol{A}}) = \mathcal{R}(\hat{\boldsymbol{a}}_k) \oplus \mathcal{R}(\hat{\boldsymbol{A}}_k) \tag{20}$$

where $\hat{\boldsymbol{a}}_k$ is the kth steering vector, $\oplus$ represents the direct sum operator, and $\hat{\boldsymbol{A}}_k$ denotes the array steering matrix without $\hat{\boldsymbol{a}}_k$. Thus the estimated covariance matrix $\hat{\boldsymbol{R}}$ can be reexpressed as

$$\begin{aligned}\hat{\boldsymbol{R}} &= [\boldsymbol{a}_k, \boldsymbol{A}_k]\begin{bmatrix} \hat{r}_{sk} & \hat{\boldsymbol{\rho}}^T \\ \hat{\boldsymbol{\rho}}^* & \hat{\boldsymbol{R}}_{Ak}\end{bmatrix}\begin{bmatrix}\boldsymbol{a}_k^H \\ \boldsymbol{A}_k^H\end{bmatrix} + \hat{\boldsymbol{R}}_w \\ &= \hat{r}_{sk}\boldsymbol{a}_k\boldsymbol{a}_k^H + \boldsymbol{a}_k\hat{\boldsymbol{\rho}}^T\boldsymbol{A}_k^H \\ &\quad + \boldsymbol{A}_k\hat{\boldsymbol{\rho}}^*\boldsymbol{a}_k^H + \boldsymbol{A}_k\hat{\boldsymbol{R}}_{Ak}\boldsymbol{A}_k^H + \hat{\boldsymbol{R}}_w \end{aligned}\tag{21}$$

where $\hat{\boldsymbol{\rho}} = (1/N)\sum_{n=1}^N s_k(n)\boldsymbol{s}_{Ak}(n) \neq \boldsymbol{0}_{(K-1)\times 1}$, $\boldsymbol{s}_{Ak}(n)$ denotes the signal vector without signal $s_k(n)$, and $\hat{\boldsymbol{R}}_{Ak}$ denotes the signal covariance corresponding to $\boldsymbol{A}_k$. Then, to deal with the second and third items in (21), we have K new oblique projection operators as [19]

$$\hat{\boldsymbol{E}}_{A_k|a_k}^{(i)} \triangleq \hat{\boldsymbol{A}}_k(\hat{\boldsymbol{A}}_k^H\hat{\boldsymbol{\Pi}}_{\hat{a}_k}^{\perp}\hat{\boldsymbol{A}}_k)^{-1}\hat{\boldsymbol{A}}_k^H\hat{\boldsymbol{\Pi}}_{\hat{a}_k}^{\perp} \tag{22}$$

where $k = 1, \cdots, K$ and $\hat{\boldsymbol{\Pi}}_{\hat{a}_k}^{\perp} \triangleq \boldsymbol{I}_{2M+1} - \hat{\boldsymbol{a}}_k(\hat{\boldsymbol{a}}_k^H\hat{\boldsymbol{a}}_k)^{-1}\hat{\boldsymbol{a}}_k^H$. From (21) and (22), we obtain

$$\begin{aligned}\hat{\boldsymbol{R}}_k^{(i)} &\triangleq \left(\boldsymbol{I}_{2M+1} - \hat{\boldsymbol{E}}_{A_k|a_k}^{(i)}\right)\hat{\bar{\boldsymbol{R}}}\left(\boldsymbol{I}_{2M+1} - \hat{\boldsymbol{E}}_{A_k|a_k}^{(i)}\right)^H \\ &\approx \hat{r}_{sk}\hat{\boldsymbol{a}}_k\hat{\boldsymbol{a}}_k^H + \Delta\hat{\boldsymbol{R}}_w \end{aligned}\tag{23}$$

where

$$\Delta\hat{\boldsymbol{R}}_w \triangleq \left(\boldsymbol{I}_{2M+1} - \hat{\boldsymbol{E}}_{A_k|a_k}^{(i)}\right)\hat{\boldsymbol{R}}_w\left(\boldsymbol{I}_{2M+1} - \hat{\boldsymbol{E}}_{A_k|a_k}^{(i)}\right)^H \tag{24}$$

Obviously, when SNR is sufficiently high, the matrix $\Delta\hat{\boldsymbol{R}}_w$ is reasonable small. Then we have

$$\hat{\boldsymbol{R}}_k^{(i)} \approx \hat{r}_{sk}\hat{\boldsymbol{a}}_k\hat{\boldsymbol{a}}_k^H \tag{25}$$

Apparently, $\hat{\boldsymbol{R}}_k^{(i)}$ contains exclusive $\hat{\psi}_k - b\hat{\phi}_k$ information of the kth signal. Finally, by estimating the electric angles in Section III-A with (14)–(16), the electric angles estimates could be updated as$\{\hat{\psi}_k^{(i+1)}\}_{k=1}^K$ and $\{\hat{\phi}_k^{(i+1)}\}_{k=1}^K$ as $i = i+1$. Repeat this procedure till the difference between two consecutive iterations becomes smaller than a threshold, i.e.,

$$\sum_{k=1}^{K}\left|\hat{\psi}_k^{(i+1)} - \hat{\psi}_k^{(i)}\right| \leq \varepsilon \tag{26}$$

where ε is an arbitrary and positive small constant (e.g., $\varepsilon = 10^{-6}$), then denote $\hat{\psi}_k = \hat{\psi}_k^{(i+1)}$ and $\hat{\phi}_k = \hat{\phi}_k^{(i+1)}$ (i.e., the corresponding DOAs and ranges).

Therefore based on the above discussion, when the finite array data $\{\boldsymbol{x}(n)\}_{n=1}^N$ are available, the implementation of the proposed method can be summarized as follows:

1) Estimate the sample array covariance matrix $\hat{\boldsymbol{R}}$ with (19) and the noise variance $\hat{\sigma}^2$ with the existing method (cf. [22]).

2) Estimate the electric angles $\{\psi_k\}_{k=1}^K$ and $\{\phi_k\}_{k=1}^K$ with (14)–(16).
3) By calculating the estimated matrix $\hat{\boldsymbol{R}}_k$ with (22) and (23), update the electric angles $\{\hat{\psi}_k^{(i)}\}_{k=1}^K$ and $\{\hat{\phi}_k^{(i)}\}_{k=1}^K$.
4) If the termination condition in (26) is not satisfied, repeat Step 3 by setting $i = i + 1$; otherwise re-express the estimates $\{\hat{\psi}_k^{(i+1)}\}_{k=1}^K$ and $\{\hat{\phi}_k^{(i+1)}\}_{k=1}^K$ as $\{\hat{\psi}_k\}_{k=1}^K$ and $\{\hat{\phi}_k\}_{k=1}^K$ (i.e., the corresponding DOAs $\{\hat{\theta}_k\}_{k=1}^K$ and ranges $\{\hat{r}_k\}_{k=1}^K$).

V. STATISTICAL ANALYSIS

The asymptotic MSE expressions of the estimated DOAs and ranges of the near-field signals are given as follows.

Theorem 1: The large-sample MSEs of the estimation error $\hat{\theta}_k - \theta_k$ and $\hat{r}_k - r_k$ of the near-field signals obtained by (17) and (18) are given by

$$\mathrm{E}\{(\Delta\theta_k)^2\} = \frac{\alpha_1^2}{\cos^2(\theta_k)} E\{(\Delta\gamma_{0,k})^2\} \tag{27}$$

$$\begin{aligned}\mathrm{E}\{(\Delta r_k)^2\} = &\frac{\alpha_2^2\cos^4(\theta_k)}{4\psi_k^4}\big(E\{(\Delta\gamma_{-1,k})^2\} + E\{(\Delta\gamma_{1,k})^2\} \\ &- 2E\{\Delta\gamma_{-1,k}\Delta\gamma_{1,k}\}\big) \\ &+ \frac{\alpha_1\alpha_2^2}{\psi_k^3}\cos(\theta_k)\sin(2\theta_k)\big(E\{\Delta\gamma_{0,k}\Delta\gamma_{-1,k}\} \\ &- E\{\Delta\gamma_{0,k}\Delta\gamma_{1,k}\}\big) + \frac{4(\alpha_1\alpha_2)^4}{\psi^2}E\{(\Delta\gamma_{0,k})^2\}\end{aligned} \tag{28}$$

where $\alpha_1 = -\lambda/2\pi d$, $\alpha_2 = \pi d^2/\lambda$, $[\gamma_{0,k}, \gamma_{-1,k}, \gamma_{1,k}]^T \triangleq [\phi_k, \phi_k + \psi_k, \phi_k - \psi_k]^T$, and

$$E\{\Delta\gamma_{i,k}\Delta\gamma_{j,k}\} = \big[E\{\Delta\boldsymbol{\gamma}_i\Delta\boldsymbol{\gamma}_j\}\big]_{k,k} \tag{29}$$

where $\Delta\boldsymbol{\gamma}_i = [\Delta\gamma_{i,1}, \Delta\gamma_{i,2}, \cdots, \Delta\gamma_{i,K}]^T$ and

$$\begin{aligned}E\{\Delta\boldsymbol{\gamma}_i\Delta\boldsymbol{\gamma}_j^T\} = \frac{1}{2}\mathrm{Re}\Big\{&\boldsymbol{W}_i E\{\boldsymbol{\epsilon}_i\boldsymbol{\epsilon}_j^H\}\boldsymbol{W}_j^H \\ &-\boldsymbol{W}_i E\{\boldsymbol{\epsilon}_i\boldsymbol{\epsilon}_j^T\}\boldsymbol{W}_j^T\Big\}\end{aligned} \tag{30}$$

where $\boldsymbol{W}_i = \boldsymbol{D}_{i,0}^{-1}\boldsymbol{D}_{i,2}\boldsymbol{D}_{i,1}^{-1}(\boldsymbol{\Psi}_{i,1}^H\boldsymbol{\Psi}_{i,1})^{-1}\boldsymbol{\Psi}_{i,1}^H$, where $\big[E\{\boldsymbol{\epsilon}_i\boldsymbol{\epsilon}_j^H\}\big]_{u,v} = E\{\epsilon_{i,u}\epsilon_{j,v}^*\}$, $\big[E\{\boldsymbol{\epsilon}_i\boldsymbol{\epsilon}_j^T\}\big]_{u,v} = E\{\epsilon_{i,u}\epsilon_{j,v}\}$, and

$$\begin{aligned}E\{\epsilon_{i,u}\epsilon_{j,v}^*\} = &\frac{\sigma^4}{N}\mathrm{tr}\{\boldsymbol{M}_{i,u}\boldsymbol{M}_{j,v}^H\} \\ &+ \frac{\sigma^4}{2N}\frac{1}{2M+1-2K}\mathrm{tr}\{\boldsymbol{M}_{i,u}\}\mathrm{tr}\{\boldsymbol{M}_{j,v}^H\} \\ &+ \frac{\sigma^4}{N}\mathrm{tr}\{\boldsymbol{M}_{i,u}\bar{\boldsymbol{R}}\boldsymbol{M}_{j,v}^H + \boldsymbol{M}_{i,u}\boldsymbol{M}_{j,v}^H\bar{\boldsymbol{R}}\}\end{aligned} \tag{31}$$

$$\begin{aligned}E\{\epsilon_{i,u}\epsilon_{j,v}\} = &\frac{\sigma^4}{N}\mathrm{tr}\{\boldsymbol{M}_{i,u}\boldsymbol{M}_{j,v}^T\} \\ &+ \frac{\sigma^4}{2N}\frac{1}{2M+1-2K}\mathrm{tr}\{\boldsymbol{M}_{i,u}\}\mathrm{tr}\{\boldsymbol{M}_{j,v}^T\} \\ &+ \frac{\sigma^4}{N}\mathrm{tr}\{\boldsymbol{M}_{i,u}\bar{\boldsymbol{R}}\boldsymbol{M}_{j,v}^T + \boldsymbol{M}_{i,u}\boldsymbol{M}_{j,v}^T\bar{\boldsymbol{R}}\}\end{aligned} \tag{32}$$

$$\boldsymbol{D}_{i,0} = \mathrm{diag}\{\sigma_{s_1}^2 e^{-j(2M-|i|)\gamma_{i,1}}, \cdots, \sigma_{s_K}^2 e^{-j(2M-|i|)\gamma_{i,K}}\} \tag{33}$$

$$\boldsymbol{D}_{i,1} = \mathrm{diag}\{\alpha_{i,1}, \alpha_{i,2}, \cdots, \alpha_{i,K}\} \tag{34}$$

$$\boldsymbol{D}_{i,2} = \mathrm{diag}\{e^{j(\phi_1 - i\psi_1)}, e^{j(\phi_2 - i\psi_2)}, \cdots, e^{j(\phi_K - i\psi_K)}\} \tag{35}$$

$$\boldsymbol{\Psi}_{i,1} = \begin{bmatrix} e^{-2j\gamma_{i,1}}, & e^{-2j\gamma_{i,2}}, & \cdots, & e^{-2j\gamma_{i,K}} \\ e^{-4j\gamma_{i,1}}, & e^{-4j\gamma_{i,2}}, & \cdots, & e^{-4j\gamma_{i,K}} \\ \vdots & \vdots & \ddots & \vdots \\ e^{-2Lj\gamma_{i,1}}, & e^{-2Lj\gamma_{i,2}}, & \cdots, & e^{-2Lj\gamma_{i,K}} \end{bmatrix} \tag{36}$$

where $\boldsymbol{M}_{iu} \triangleq (\boldsymbol{e}_u^T \otimes \boldsymbol{I}_{2M+1})\boldsymbol{C}_i(\bar{\boldsymbol{a}}_i \otimes \boldsymbol{I}_{2M+1})$, $\bar{\boldsymbol{R}} = \boldsymbol{R} - \sigma^2\boldsymbol{I}_{2M+1}$, and

$$\boldsymbol{C}_i = \begin{bmatrix} \boldsymbol{e}_{2M+2-\bar{K}-i_1}\boldsymbol{e}_{\bar{K}+i_2}^T & \cdots & \boldsymbol{e}_{2M+1-i_1}\boldsymbol{e}_{1+i_2}^T \\ \boldsymbol{e}_{2M+1-\bar{K}-i_1}\boldsymbol{e}_{\bar{K}+1+i_2}^T & \cdots & \boldsymbol{e}_{2M-i_1}\boldsymbol{e}_{2+i_2}^T \\ \vdots & \ddots & \vdots \\ \boldsymbol{e}_{1-i_1}\boldsymbol{e}_{2M+1+i_2}^T & \cdots & \boldsymbol{e}_{\bar{K}-i_1}\boldsymbol{e}_{2M+2+i_2}^T \end{bmatrix} \tag{37}$$

Proof: Omitted. ∎

VI. SIMULATION RESULTS

The performance of proposed method is verified using a ULA consisting of $2M + 1 = 9$ sensors with element spacing $d = \lambda/4$. Two signals with equal power arrive from the direction $(-6°, 2.5\lambda)$ and $(13°, 2.7\lambda)$. The maximum number of iterations is set as 50 and the iteration threshold is set as 10^{-6} respectively. Meanwhile, the behavior of WLPM [17], GEMM, and the Cramer-Rao lower bound (CRB) [17] are also presented, while SNR is defined as the ratio of the signal power to the noise variance at each sensor, and the root square errors (RMSEs) of the the DOA and range are calculated respectively. The results in each of the examples below are obtained from 1000 independent Monte Carlo trails.

1) Example 1: In the first experiment, the number of snapshots is set as $N = 200$, and SNR varies from -10 dB to 40 dB. The RMSEs of the DOAs and ranges estimates versus SNR are shown in Fig. 1. It shows that the performance of the proposed method generally behaves better than both WLPM and GEMM. Furthermore, when the number of iteration is sufficient large, the saturation problem is solved effectively. The performance of the ranges estimation of the proposed method is better than WLPM and agrees with the theoretical analysis.

2) Example 2: In the second experiment, SNR is fixed to 10 dB, and the number of snapshots varies from 10 to 1000. The RMSEs of the DOAs and ranges estimates versus the number of snapshots are shown in Fig. 2. It can be observed that the performance of the proposed approach gains significantly than both WLPM and GEMM for DOAs estimation. For range estimates, the proposed method behaves much better than WLPM, and it stays very close to the theoretical analysis and CRB, which demonstrates the robustness and effectiveness of the proposed method.

VII. CONCLUSION

In this paper, a new LP approach based on truncated SVD was proposed for localization of multiple near-field signals impinging on a symmetrical ULA, and an alternating iterative

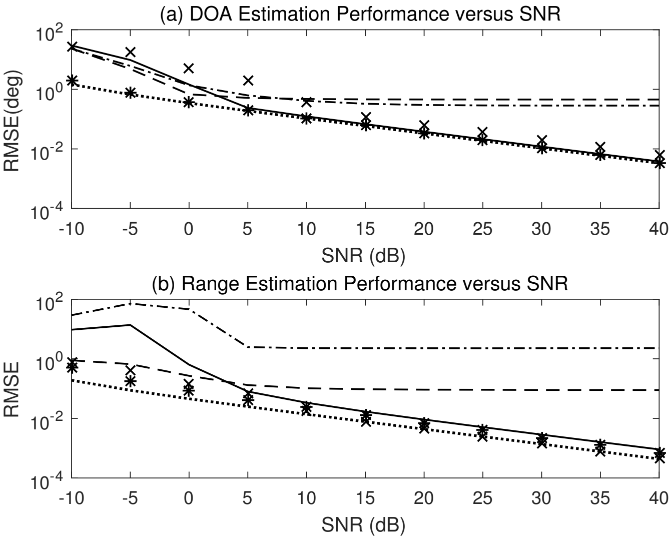

Fig. 1. RMSEs of the (a) DOA and (b) range estimates versus the SNR (dash-dotted line: WLPM; "×": GEMM; dashed line: the proposed method w/o iteration; solid line: the proposed method; "∗":theoretical RMSE of the proposed method; dash-dotted line: CRB) for Example 1.

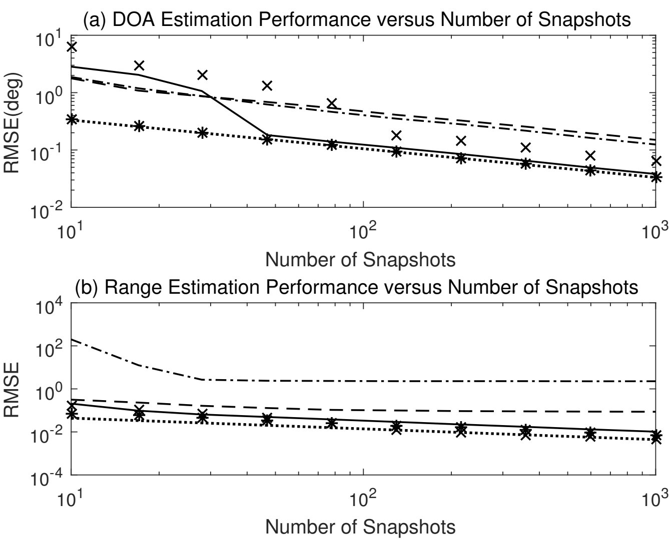

Fig. 2. RMSEs of the (a) DOA and (b) range estimates versus the number of snapshots (dash-dotted line: WLPM; "×": GEMM; dashed line: the proposed method w/o iteration; solid line: the proposed method; "∗":theoretical RMSE of the proposed method; dash-dotted line: CRB) for Example 2.

scheme was also presented as a measure against the impact of finite array data for improving the estimation accuracy of the location parameters and overcoming the "saturation behavior" encountered in most of localization methods of the near-field signals. Furthermore, the asymptotic MSE expressions of the estimation errors were derived for two location parameters. Finally, the effectiveness and the theoretical analysis were verified through numerical examples.

References

[1] H. Krim and M. Viberg, "Two decades of array signal processing research: The parametric approach," *IEEE Signal Process. Mag.*, vol. 13, no. 4, pp. 67-94, 1996.

[2] P. R. P. Hoole, *Smart Antennas and Signal Processing for Communications, Wireless and Radar Systems.* Southampton, U.K.: WIT Press, 2001

[3] A. J. Weiss and B. Friedlander, "Range and bearing estimation uisng polynomial rooting," *IEEE J. Oceanic Eng.*, vol. 18, no. 2, pp. 130-137, 1993.

[4] J. C. Chen, R. E. Hudson, and K. Yao, "Maximum-likelihood source localization and unknown sensor location estimation for wideband signals in the near-field," *IEEE Trans. Signal Process.*, vol. 50, no. 8, pp. 1843-1854, 2002.

[5] A. L. Swindlehurst and T. Kailath, "Passive direction-of-arrival and range estimation for near-field sources," in *Proc. 1988 IEEE 4th ASSP Workshop Spec. Est. Mod.*, pp. 123-128, Minneapolis, MN, Aug. 1988.

[6] R. N. Challa and S. Shamsunder, "High-order subspace-based algorithms for passive localization of near-field sources," in *Proc. 1995 IEEE 29th Asilomar Conf. Signals, Syst., Comput.*, Pacific Grove, CA, vol. 2, pp. 777-781, Nov. 1995

[7] R. O. Schmidt, "Multiple emitter location and signal parameters estimation," *IEEE Trans. Antennas Propag.*, vol. 34, no. 3, pp. 267-280, 1986.

[8] R. Roy and T. Kailath, "ESPRIT-estimation of signal parameters via rotational invariance techniques," *IEEE Trans. Acoust., Speech, Signal Process.*, vol. 37, no. 7, pp. 984-995, 1989.

[9] J. Liang and D. Liu, "Passive localization of near-field sources using cumulant," *IEEE Sensors J.*, vol. 9, no. 8, pp. 953-960, 2009.

[10] J. Li, Y. Wang, C. Le Bastard, G. Wei, B. Ma, M. Sun, and Z. Yu, "Simplified high-order DOA and range estimation with linear antenna array," *IEEE Comm. Lett.*, vol. 21, no. 1, pp. 76-79, 2017.

[11] J. H. Lee and C. H. Tung, "Estimating the bearings of near-field cyclostationary signals," *IEEE Trans. Signal Process.*, vol. 50, pp. 110-118, 2002.

[12] N. Kabaoglu, H. A. Cirpan, E. Cekli, and S. Paker, "Deterministic maximum likelihood approach for 3-D near field source localization," *Int. J. Electron. Commun. (AE)*, vol. 57, no. 5, pp. 345-350, 2003.

[13] N. Kabaoglu, H. A. Cirpan, and S. Paker, "Unconditional maximum likelihood approach for localization of near-field sources in 3D space," in *Proc. 4th IEEE Int. Symp. Signal Process. Information Technology*, pp. 233-237, 2004.

[14] D. Starer and A. Nehorai, "Passive localization of near-field sources by path following," *IEEE Trans. Signal Process.*, vol. 42, no. 3, pp. 677-680, 1994.

[15] R. Boyer and J. Picheral, "Second-order near-field localization with automatic paring operation," in *Proc. IEEE Int. Conf. on Acoustics, Speech and Signal Process.*, pp. 2569-2572, Las Vegas, NV, 2008.

[16] W. Zhi and M. Y. W. Chia, "Near-field source localization via symmetric subarrays," *IEEE Signal Process. Lett.*, vol. 14, pp. 409-412, 2007.

[17] E. Grosicki, K. Meraim, and Y. Hua, "A weighted linear prediction method for near-field source localization," *IEEE Trans. Signal Process.*, vol. 53, pp. 3651-3660, 2005.

[18] C. C. Yeh, Y. Hong, and D. Ucci, "The effect of a finite distance source on an Applebaum array", *IEEE Trans. on Antennas and Propag.*, vol. 33, no. 9, pp. 1003-1008, Sep 1985.

[19] R.T. Behrens and L.L. Scharf, "Signal processing applications of oblique projection operators," *IEEE Trans. Signal Process.*, vol. 42, no. 6, pp. 1413-1424, 1994.

[20] D. W. Tufts and R. Kumaresan, "Estimation of frequencies of multiple sinusoids: Making linear prediction perform like maximum likelihood," *Proc. IEEE*, vol. 70, no. 9, pp. 975-989, 1982.

[21] R. Kumaresan and D. W. Tufts, "Estimating the angles of arrival of multiple plane waves," *IEEE Trans. Aerosp. Electron. Syst.*, vol. 19, pp. 134-139, 1983.

[22] J. Sanchez-Araujo and S. Marcos, "Statistical analysis of the propagator method for DOA estimation without eigendecomposition," in *Proc. IEEE 8th Workshop Statistical Signal and Array Process.*, pp. 570-573, Corfu, Greece, Jun. 1996.

[23] H. Tao, J. Xin, J. Wang, N. Zheng, and A. Sano, "Two-dimensional direction estimation for a mixture of noncoherent and coherent signals," *IEEE Trans. Signal Process.*, vol. 63, no. 2, pp. 318-333, 2015.

[24] J. Xin and A. Sano, "Linear prediction approach to direction estimation of cyclostationary signals in multipath environment," *IEEE Trans. Signal Process.*, vol. 49, no. 4, pp. 710-720, 2001.